CrossMark

Synthesis and Characterization of New Triazole Derivatives as Corrosion Inhibitors of Carbon Steel in Acidic Medium

Salima K. Ahmed[1] · Wassan B. Ali[1] · Anees A. Khadom[2]

Abstract

Six novel triazole derivatives were synthesized from some substituted benzoic acid with thiocarbohydrazide by grinding method. The synthesized compounds were characterized by infra-red, ^{1}H, and ^{13}C-NMR spectra investigations. Synthesized triazole derivatives were tested and evaluated as corrosion inhibitors for low-carbon steel in 0.5 M HCl using weight loss technique. It was found that these compounds had a promising inhibitory action against corrosion of mild steel in acidic solution. Inhibitor with highest performance was evaluated at different temperature and inhibitor concentrations. The inhibition efficiency exceeded 96%. The excellent inhibitor performance was attributed to the formation of inhibitor adsorption films on the steel surface. The adsorption of inhibitor on steel surface followed the Langmuir adsorption isotherm. The experimental results were confirmed via theoretical quantum chemical calculations.

Keywords Triazole · Weight loss · Corrosion inhibition · Schiff bases · Acidic solution

1 Introduction

Steel can be in contact with acidic solutions during the processes of pickling, metal cleaning, oil wells acidizing, etc. This contact can be very severe and harmful to the metal surfaces. Metal surface protection against corrosion is a practical means of corrosion control in acidic solutions [1–4]. Using of organic compounds as corrosion inhibitors for metals in aqueous solutions received a great attention in the industrial processes and scientific research [5–8]. The most effective corrosion inhibitors are those compounds containing heteroatoms such as nitrogen, sulfur, oxygen, and phosphorus, as well as aromatic rings which block the active sites, decreasing the corrosion rate [9–13]. The compounds that contain both nitrogen and sulfur showed excellent inhibition performance as compared with compounds containing only nitrogen or sulfur [14, 15]. In research on organic corrosion inhibitors, attention is paid

to the mechanism of adsorption as well as the relationship between inhibitor structures and their adsorption properties. It has been observed that the adsorption depends mainly on the electronic and structural properties of the inhibitor molecule such as functional groups, steric factors, aromaticity, electron density on donor atoms and p orbital character of donating electron [16, 17]. Also, efficient inhibitors should possess plentiful p-electrons and unshared electron pairs on either nitrogen atoms or sulfur atoms of the inhibitors to the d-orbitals of iron, and by means of transference of electrons chemical adsorption may occur on the steel surface. Thus, the steel corrosion may be suppressed by the protective film on the steel surface [18]. In the selection of a suitable compound for corrosion inhibition, the geometric and the electronic properties of the compound influence the ability of the compound to cover the metal surface and the ability of the compound to react with the metal surface and therefore just bind to the metal surface. In searching for suitable organic corrosion inhibitors, several researchers have reported the role of some triazole derivatives as corrosion inhibitors on different metal surfaces and in different environments [19–22]. Therefore, Quantum chemical methods combined with experimental methods have been utilized to confirm the potential of triazole derivatives as corrosion inhibitors [21, 22]. In the present work, six triazole derivatives were

✉ Anees A. Khadom
aneesdr@gmail.com

[1] Department of Chemistry, College of Science, University of Diyala, Baquba, Diyala Governorate 32001, Iraq

[2] Department of Chemical Engineering, College of Engineering, University of Diyala, Baquba, Diyala Governorate 32001, Iraq

synthesized and tested as corrosion inhibitors of steel in acidic solution.

2 Experimental Work

2.1 Synthesis of Inhibitors

Synthesis and reaction process *were carried out in* a round-bottomed flask (100 ml) contained in a water bath. Magnetic stirrer was used to keep uniform temperature distribution inside the flask. The flask was equipped with a reflux condenser and temperature was controlled using a hot plate heater.

2-(4-Amino-5-mercapto-4H-1,2,4-triazole-3-yl)benzene-1,4-diol (T$_1$) was synthesized by the fusion of 2,5-dihydroxy benzoic acid (0.01 mol) and thiocarbohydrazide (0.015 mol) in test tube immersed in oil bath for temperature control. Hotplate was used as a source of heating (Heidolph instruments, Germany). The reaction temperature was 145 °C. The product obtained on cooling was treated in a round-bottomed flask (100 ml) with sodium bicarbonate solution at 78 °C to neutralize the unreacted carboxylic acid, if any. Water bath was used for temperature control. It was then washed with water and collected by filtration. The same apparatus and tools were used in the synthesis of other inhibitors. Furthermore, reaction temperatures for fusion process and neutralization process were same (145 and 78 °C, respectively).

4-Amino-5-(pyridine-2-yl)-4H-1,2,4-triazole-3-thiaol (T$_2$) was synthesized by the fusion of picolinic acid (0.01 mol, 1.23 g) and thiocarbohydrazide (0.015 mol, 1.59 g). The product obtained on cooling was treated with sodium bicarbonate solution to neutralize the unreacted carboxylic acid, if any. It was then washed with water and collected by filtration.

4-Amino-5-(3-(((Z)-4-nitrobenzylidene) amino)-4-((4-nitrobenzylidene) amino) phenyl)-4H-1,2,4-triazole-3-thiaol (T$_3$) was synthesized by the fusion of 3,4-bis((4-nitrobenzylidene)amino) benzoic acid (0.001 mol, 0.83 g) and thiocarbohydrazide (0.003 mol, 0.31 g). The product obtained on cooling was treated with sodium bicarbonate solution to neutralize the unreacted carboxylic acid, if any. It was then washed with water and collected by filtration.

5,5′-(((1,4-Phenylenebis(methanylylidene)) bis(azanylylidene))bis(4,1-phenylene))bis(4-amino-4H-1,2,4-triazole-3-thiol) (T$_4$) *and 4-amino-5-(4-((4-(4-amino-5-mercapto-4H-1,2,4-triazol-3-yl)benzylidene)amino) phenyl)-4H-1,2,4-triazole-3-thiaol* (T$_5$) were synthesized by the fusion of compounds substituted benzoic acid (0.002 mol) and thiocarbohydrazide (0.006 mol). The product obtained on cooling was treated with sodium bicarbonate solution to neutralize the unreacted carboxylic acid, if any. It was then washed with water and collected by filtration.

4-((4-(4-Amino-5-mercapto-4H-1,2,4-triazole-3-yl) benzylidene)amino)-1,5-dimethyl-2-phenyl-1,2-dihydro-3H-pyrazol-3-one (T$_6$) was synthesized by the fusion of compound [T$_5$] (0.002 mol, 0.67 g) and thiocarbohydrazide (0.003 mol, 0.31 g). The product obtained on cooling was treated with sodium bicarbonate solution to neutralize the unreacted carboxylic acid, if any. It was then washed with water and collected by filtration.

For all above, the completion of the reaction and the purity of the compound were checked by thin-layer chromatography (TLC, mobile phase hexane:ethyl acetate 1:2). The product was recrystallized from appropriate solvent to afford the title compound [23, 24]. Figure 1 shows the synthesis scheme of inhibitors (T1–T6).

2.2 Quantum Chemical Calculations

The theoretical calculations of quantum chemical have been widely employed to simulate the corrosion inhibition process. The structural parameters, highest occupied molecular orbital, lowest unoccupied molecular orbital, dipole moment (μ), and fraction of electron transferred, were calculated and optimized by *ChemOffice* version 14 software.

2.3 FTIR and NMR Analysis

Fourier transform infra-red (FTIR) spectra were verified in an PerkinElmer Spectrum type 65, spectrophotometer (Germany), which performed from 400 to 4000 cm^{-1}, using the KBr disk technique, and nuclear magnetic resonance, 1H- and 13C-NMR spectroscopy, 400 MHz (Bruker, Germany), were used in the process of analysis and diagnosis of corrosion inhibitors.

2.4 Weight Loss Measurements

Low-carbon steel test sample has the following chemical compositions (wt%): 0.1 C, 0.335 Mn, 0.033 Si, 0.0067 S, 0.0056 P, 0.057 Al, 0.0476 Cu, 0.0201 Cr, 0.001 Co, 0.0007 Ti, and the balance is Fe. Rectangular test samples are with dimensions of 3 cm × 1 cm × 0.1 cm exposing an approximated surface area of 6.8 cm^2. Prior to each measurement, the steel sample was abraded with emery papers with grade of 400–1000, washed ultrasonically with distilled water (Distilled by Simtronics Water Distillation Unit, India), acetone, and alcohol, dried under dry air, and then kept in desiccators over silica gel bed until use. The dimensions of each sample were measured with a vernier to 2nd decimal of millimeter and accurately weighted to the 4th decimal of gram. Testing electrolyte of 0.5 M HCl aqueous solution was prepared by diluting Analar Grade 37% hydrochloric acid with ultra-pure water. The metal samples were completely immersed each in 500 ml of uninhibited and inhibited
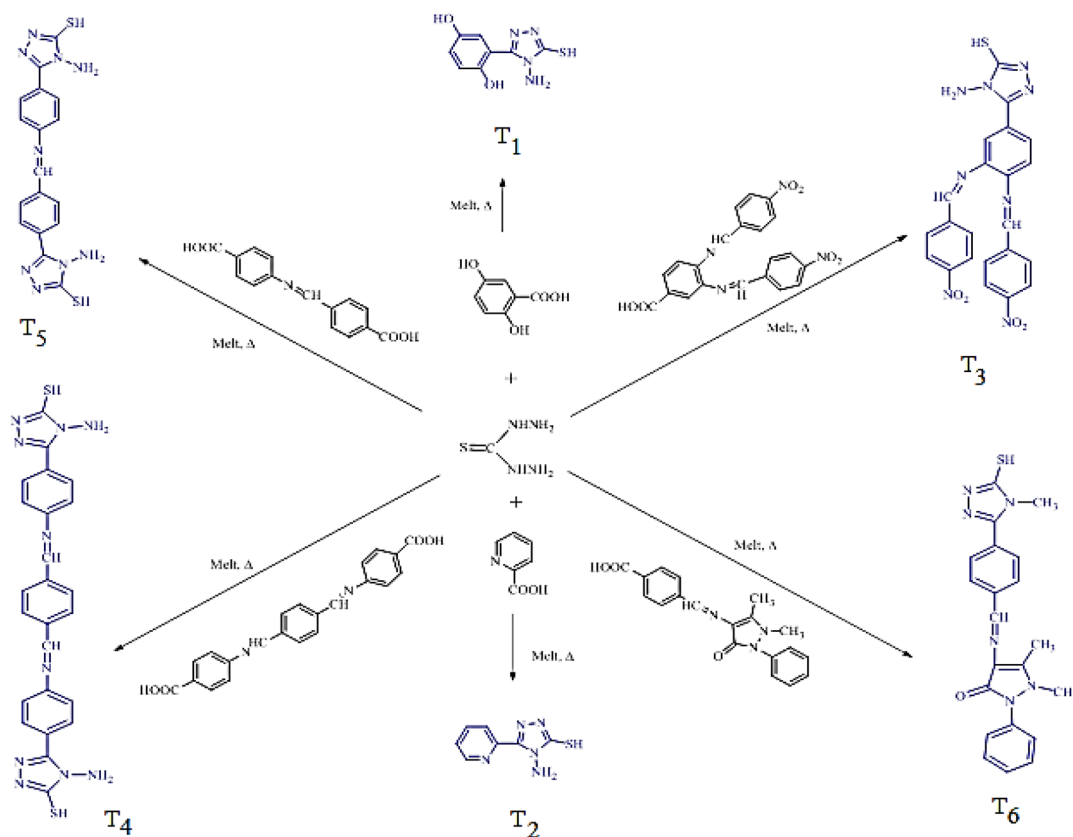
**Fig. 1** Synthesis scheme of inhibitors (T_1–T_6)

0.5 M HCl solution contained in a conical flask. Water bath was used for temperature control. They were exposed for a period of 3 h at the desired temperature and inhibitor concentration. Then the metal samples were cleaned, washed with running tap water followed by distilled water, dried with clean tissue, and then immersed in acetone and alcohol and dried again. Weight losses in g/m^2/day (gmd) were determined in the presence and absence of inhibitor. At the beginning, all inhibitors were tested at inhibitor concentration of 0.001 M and 30 °C to select the best one. Then, the inhibitor with higher efficiency was evaluated at different temperatures (20, 30, 40, and 50 °C) and inhibitor concentration of 1×10^{-3}, 2×10^{-3}, 3×10^{-3}, and 4×10^{-3} M. All measurements were performed for three times to obtain a satisfactory reproducibility.

3 Results and Discussion

3.1 Diagnoses of Inhibitors

FTIR spectra and nuclear magnetic resonance, 1H- and 13C-NMR spectroscopy were used in the process of analysis and diagnosis of corrosion inhibitors. Figures 2 and 3 show FTIR and NMR spectrum of inhibitors. The active groups and specifications were evaluated. For T_1 the observed values of were OH (3568), NH$_2$ (3356), N–H$_{str}$ (3283), aromatic C–H$_{str}$ (3173), C=N$_{str}$ (1654), aromatic C=C$_{str}$ (1566, 1497), C=S (1241). The spectrum of ^{1}H-NMR to compound appears to show the following data: 12.5 (S, 1H, OH), 8.4 (S, 1H, SH), 6.02–7.1 (4H, Aromatic H), 5.2 (S, 2H, NH$_2$). T_2 shows NH$_2$ (3432–3323), N–H$_{str}$ (3178), aromatic C–H$_{str}$ (3087), C=N$_{str}$ (1636), aromatic C=C$_{str}$ (1576–1451), C=S (1272). The spectrum of ^{1}H-NMR (400 MHz, d6-DMSO, ppm) to compound (S_6) appears to show the following data: δH = 8.7 (S, 1H, SH), 8.6 (S, 1H, N=CH), 7.5–8.1 (3H, Aromatic H), 5.3 (S, 2H, NH$_2$). The following specifications were observed for T_3: NH$_2$ (3480–3422), N–H$_{str}$ (3071), aromatic C–H$_{str}$ (3001), aliphatic C–H$_{str}$ (2942), C=N$_{str}$ (1617), C=C$_{str}$ (1445), C=S (1241). The spectrum of ^{1}H-NMR (400 MHz, d6-DMSO, ppm) to compound (S_{14}) appears to show the following data: δH = 10.5 (S, 1H, SH), 8.3 (S, 2H, N=CH), 7.9–8.2 (7H, Aromatic H), 5.8 (S, 2H, NH$_2$). For T_4 NH$_2$ (3483–3418), N–H$_{str}$ (3134), aromatic C–H$_{str}$ (3011), C=N$_{str}$ (1614), C=C$_{str}$ (1505–1414), C=S (1323). The spectrum of ^{1}H-NMR (400 MHz, d6-DMSO, ppm) to compound T_4 appears to show the following data: δH = 10.7 (S, 1H, SH), 8.7 (S, 2H, N=CH), 7.1–8.3 (8H, Aromatic H) 5.5 (S, 2H, NH$_2$). ^{13}C-NMR (400 MHz,

Fig. 2 FTIR spectrum of inhibitors (T_1–T_6)
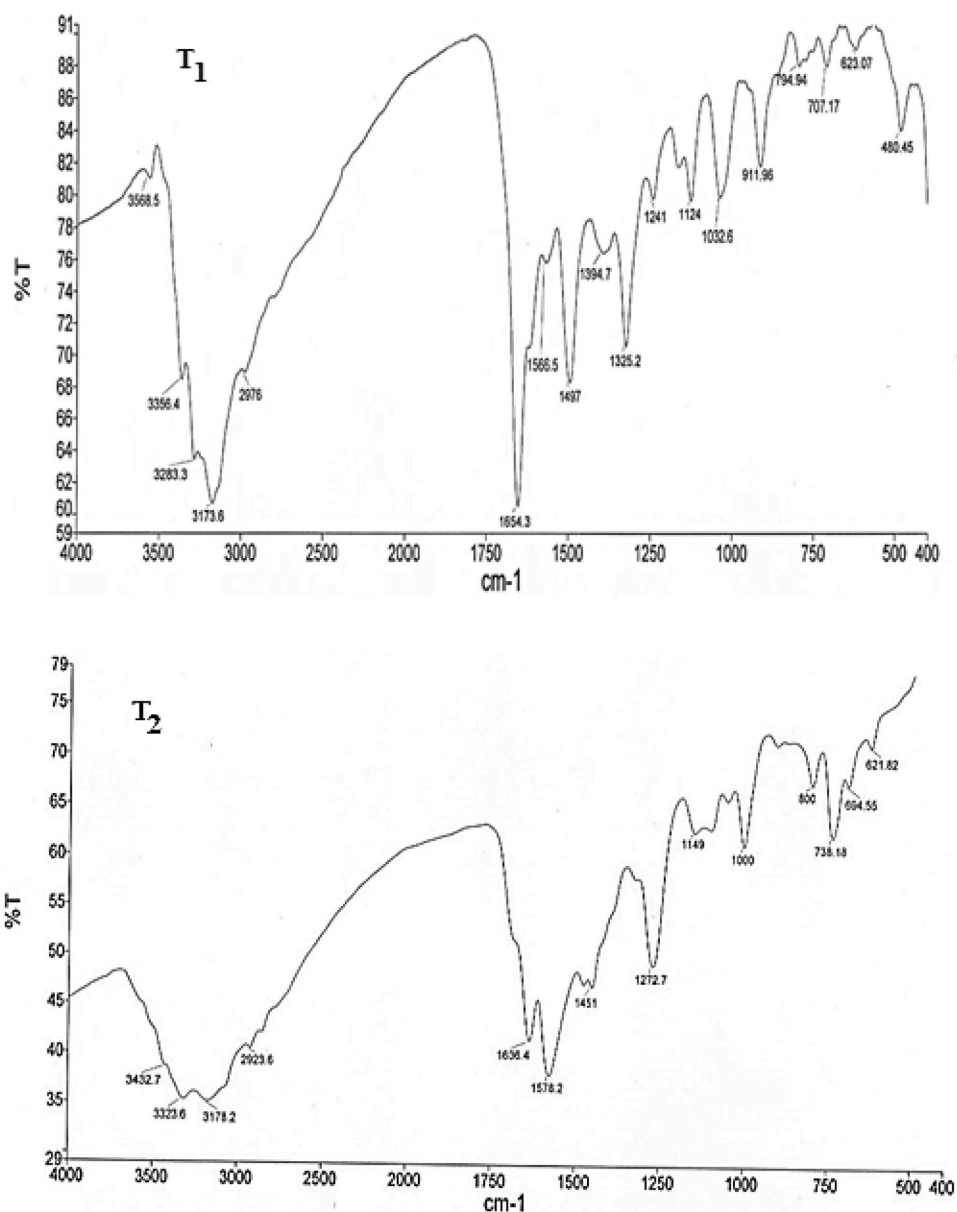
d6-DMSO, ppm): $\delta C = 164$ (CH=N) 135 (N–C–N), 149, 143, 126 (Ar–CH). However, the specifications of T_5 are: NH_2 (3276–3166), N–H_{str} (3128), aromatic C–H_{str} (2995), C=N_{str} (1588), C=C_{str} (1504–1434), C=S (1237), yield: 70%. The spectrum of ^{1}H-NMR (400 MHz, d6-DMSO, ppm) to compound (S_{17}) appears to show the following data: $\delta H = 10.9$ (S, 1H, SH), 8.7 (S, 2H, N=CH), 7.6–8.2 (4H, Aromatic H) 5.5 (S, 2H, NH_2). ^{13}C-NMR (400 MHz, d6-DMSO, ppm): $\delta C = 167$ (CH=N), 131 (N–C–N), 149, 142, 138, 129, 128, 125 (Ar–CH). The following are specifications of T_6: NH_2 (3374–3287), N–H_{str} (3185), aromatic C–H_{str} (2931), C=N_{str} (1596), C=C_{str} (1498–1443), C=S (1309), yield: 64%. The spectrum of ^{1}H-NMR (400 MHz, d6-DMSO, ppm) to compound T_6 appears to show the following data: $\delta H = 9.6$ (S, 1H, SH), 8.3 (S, 2H, N=CH), 7.3–7.9 (4H, Aromatic H), 5.5 (S,

2H, NH_2), 2.1 (S, 6H, 2CH_3). Table 1 shows the summary of inhibitor physical properties.

3.2 Weight Loss Measurements

Table 2 summarizes the results of weight loss technique of the low-carbon steel alloy corrosion in 0.5 M hydrochloric acid solution at 30 °C and 0.001 M inhibitor concentration. The values of corrosion rate were evaluated using the following equation [25]:

$$CR = \frac{\text{weight loss (g)}}{\text{area (m}^2) \times \text{time (day)}}. \tag{1}$$

Fig. 2 (continued)
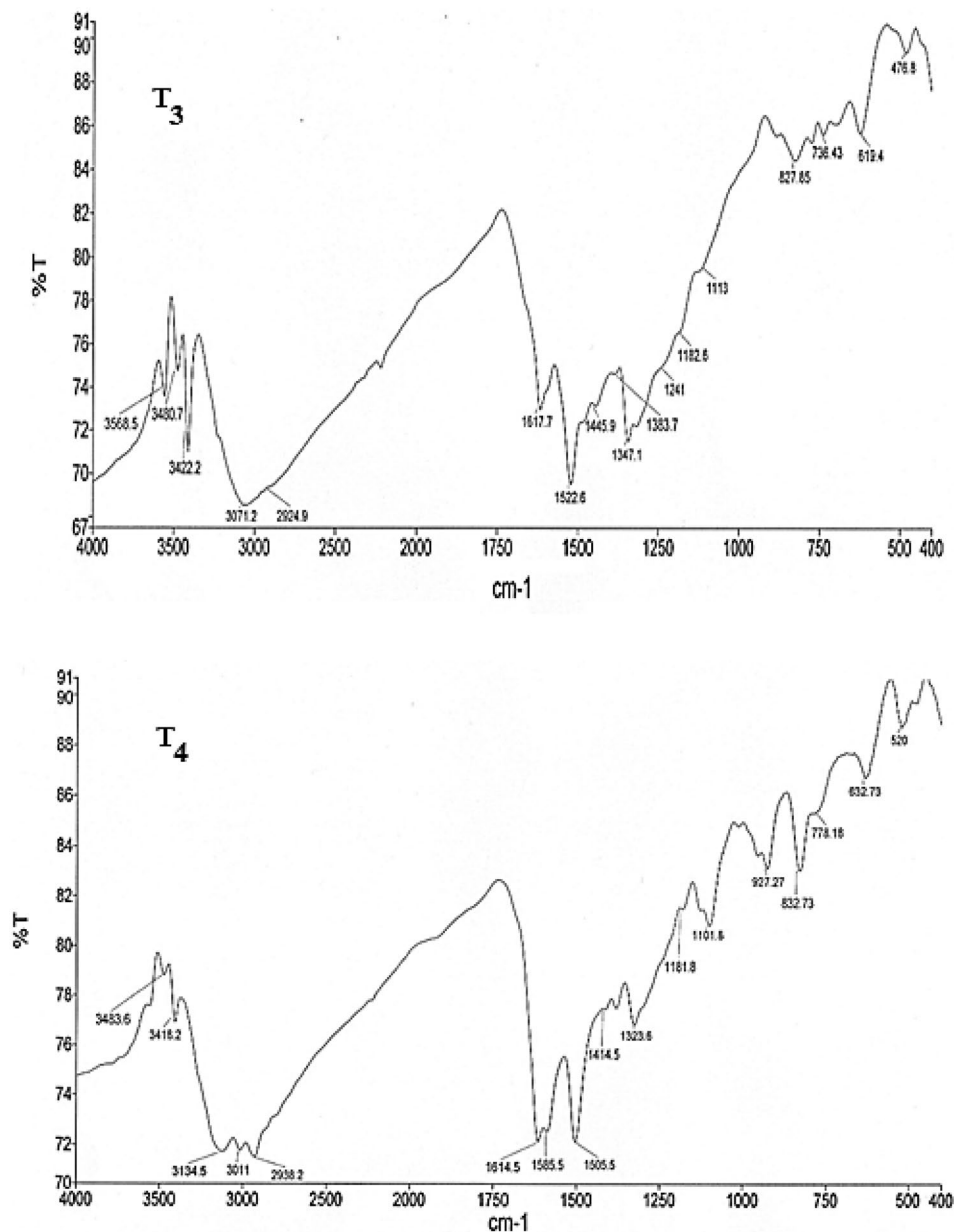
From the corrosion rate, the percentage inhibition efficiency of weight loss experiments (%IE) was calculated using the following equation [26]:

$$\%\mathrm{IE} = \frac{\mathrm{CR_{uninibit} - CR_{inhibit}}}{\mathrm{CR_{uninhibit}}} \times 100, \tag{2}$$

where $\mathrm{CR_{uninhibit}}$ and $\mathrm{CR_{inhibit}}$ are the corrosion rates in the absence and presence of inhibitors, respectively. Table 2 shows that inhibitor efficiency ranged from 72.89 to 81.08%. T_4 shows the higher performance. In order to have a clear vision of T_4 behavior, the effects of inhibitor concentration and temperature were studied. The results are shown in Table 3. Corrosion rate increased with increase

of temperature and decrease of inhibitor concentration, while inhibitor efficiency increased with the increasing inhibitor concentration and temperature. Tezcan et al. [27] investigated newly synthesized sulfur containing Schiff base (4-((thiophene-2-ylmethylene)amino)benzamide) compound. Inhibition performance on mild steel in 1.0 M HCl solution was studied. The results showed the highest inhibitor efficiency of 96.8%. Chaitra et al. [28] studied the effect of newly synthesized thiazole hydrazones on the corrosion of mild steel in 0.5 M hydrochloric acid. Adsorption of the inhibitors followed Langmuir isotherm and addition of inhibitors simultaneously decreased corrosion rate. Messali et al. [29] studied the inhibition effect and adsorption behavior of 4-((2,3-dichlorobenzylidene)

Fig. 2 (continued)
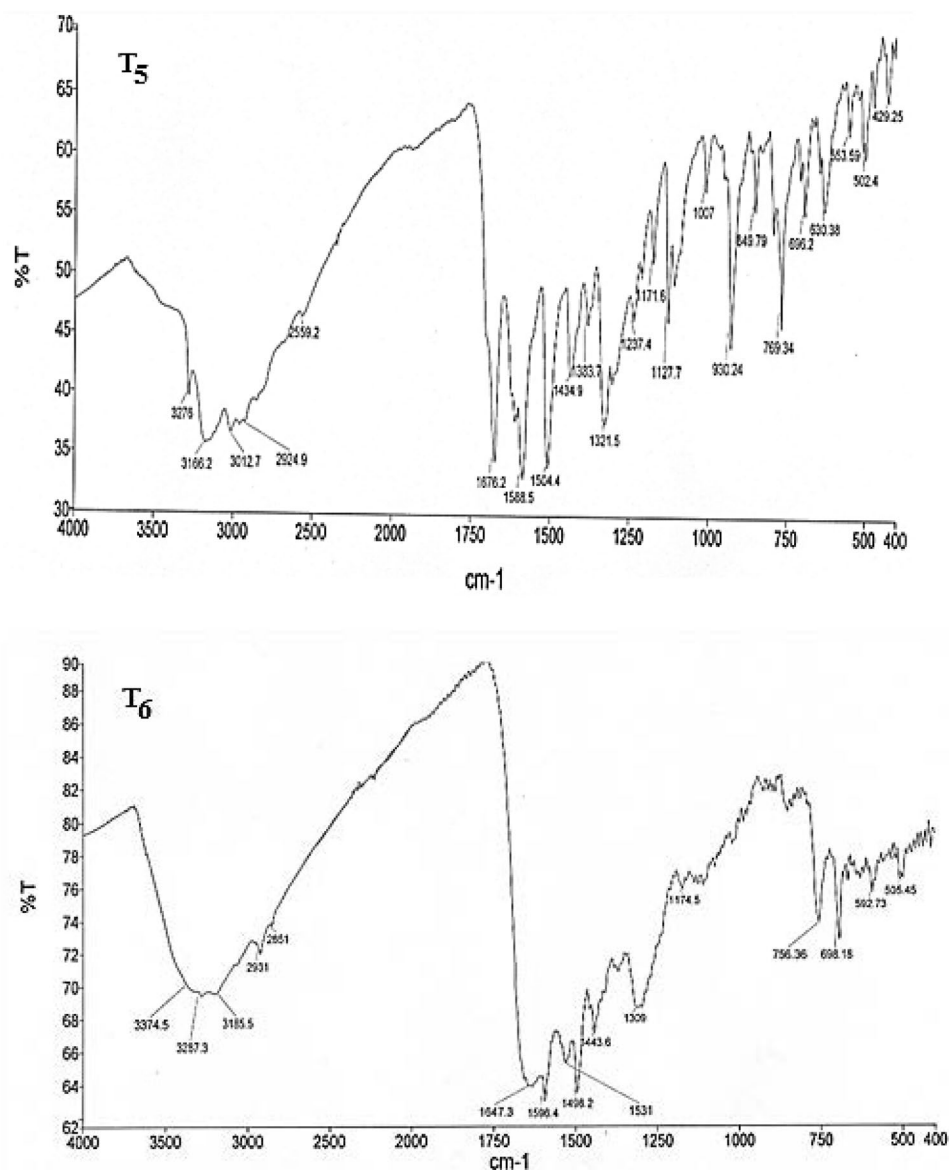
amino)-3-methyl-1H-1,2,4-triazole-5(4H)-thione on mild steel in 1 M HCl solution. The inhibitor can be adsorbed onto surface by both physical and chemical means obeying Langmuir adsorption isotherm.

3.3 Effect of Inhibitor Concentration and Adsorption Studies

As shown in Table 3, at specific experimental temperature, corrosion rate of steel decreases with an increase in T_4 concentration. Values of inhibitor efficiency increase with the increasing T_4 concentration and approach the maximum value of 96.02% at higher level of temperature and inhibitor concentration. This increase in inhibitor performance with temperature is apparently due to an increase in chemisorption of the inhibitor. Crucial step in the action of

inhibitor behavior in acidic media is commonly agreed to be the adsorption on the metal surface. This includes the assumption that the corrosion reactions are prevented from occurring over the area or active sites of the metal surface protected by adsorbed inhibitor molecules, whereas these corrosion reactions occurred generally on the inhibitor-free active sites [30]. The surface coverage ($\Theta = \%IE/100$) data are very valuable in discussing the adsorption features. Surface covered is related to the concentration of inhibitor at constant temperature by well-known adsorption isotherm relationships that are evaluated at equilibrium condition. The dependence of θ on the concentration of T_4 concentration was tested graphically by fitting it to Langmuir adsorption isotherm that assumes a metal surface contains a fixed number of adsorption sites and each site takes only one adsorbed molecule. Figure 4 shows
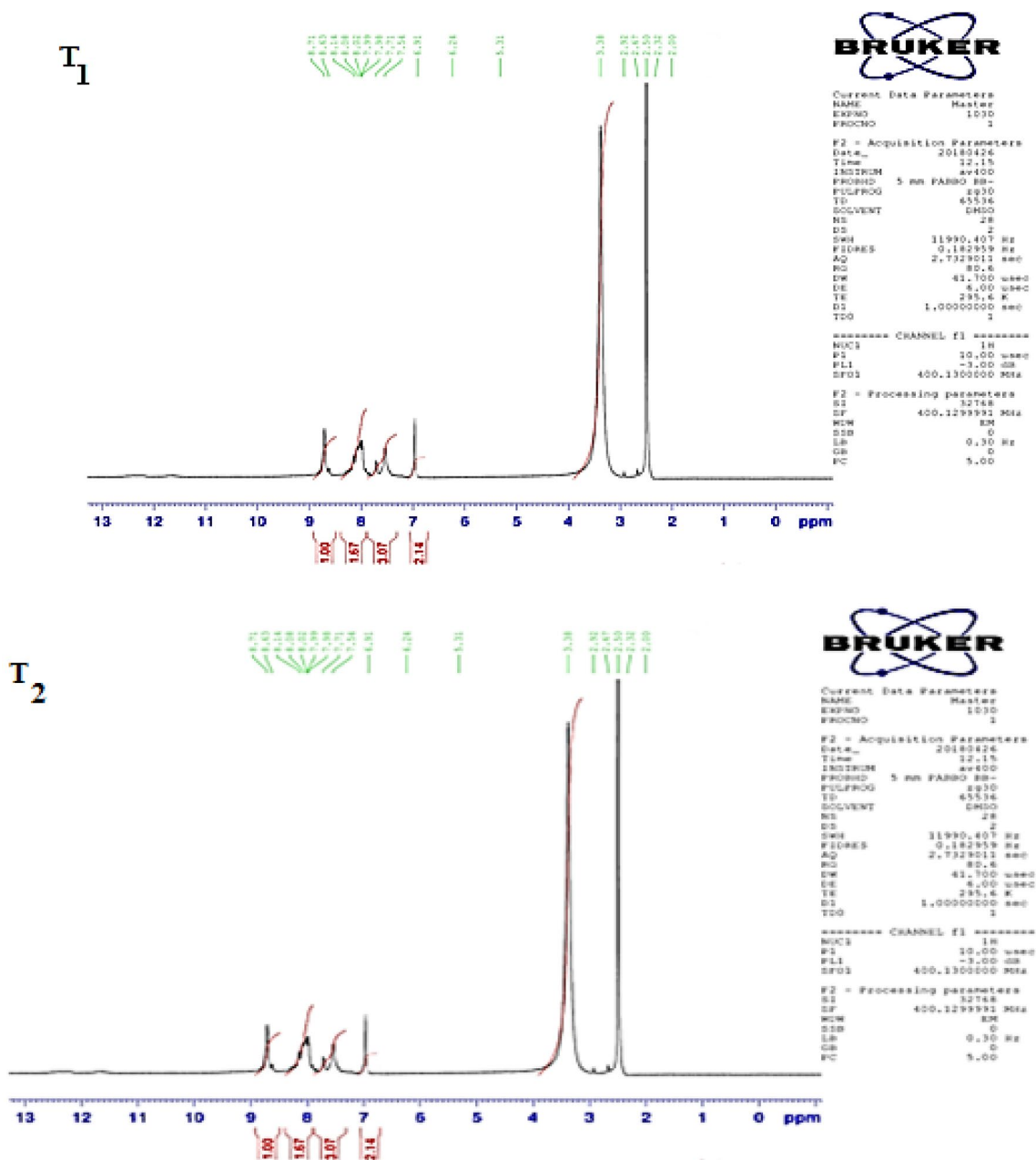
Fig. 3 NMR spectrum of inhibitors (T$_1$–T$_6$)

linear plots for C/Θ versus C with average $R^2 = 0.99$ correlation coefficient, suggesting that the adsorption follows the Langmuir adsorption isotherm [31]:

$$\frac{C}{\theta} = \frac{1}{K} + C, \tag{3}$$

where C is the inhibitor concentration and K is the adsorption equilibrium constant, representing the degree of adsorption; in other words, the higher the value of K specifies that the T$_4$ molecules is strongly adsorbed on the metal surface. The slops of Langmuir adsorption lines are near unity meaning that each inhibitor molecule occupies one active site on the metal surface.

The standard adsorption free energy (ΔG_{ads}) was calculated using the following equation [31]:

$$K = \frac{1}{55.5} \exp\left(-\frac{\Delta G_{ads}}{RT}\right), \tag{4}$$

where 55.5 is the concentration of water in solution expressed in molar, R is the gas constant, and T is the absolute temperature. Table 4 shows the adsorption parameters.
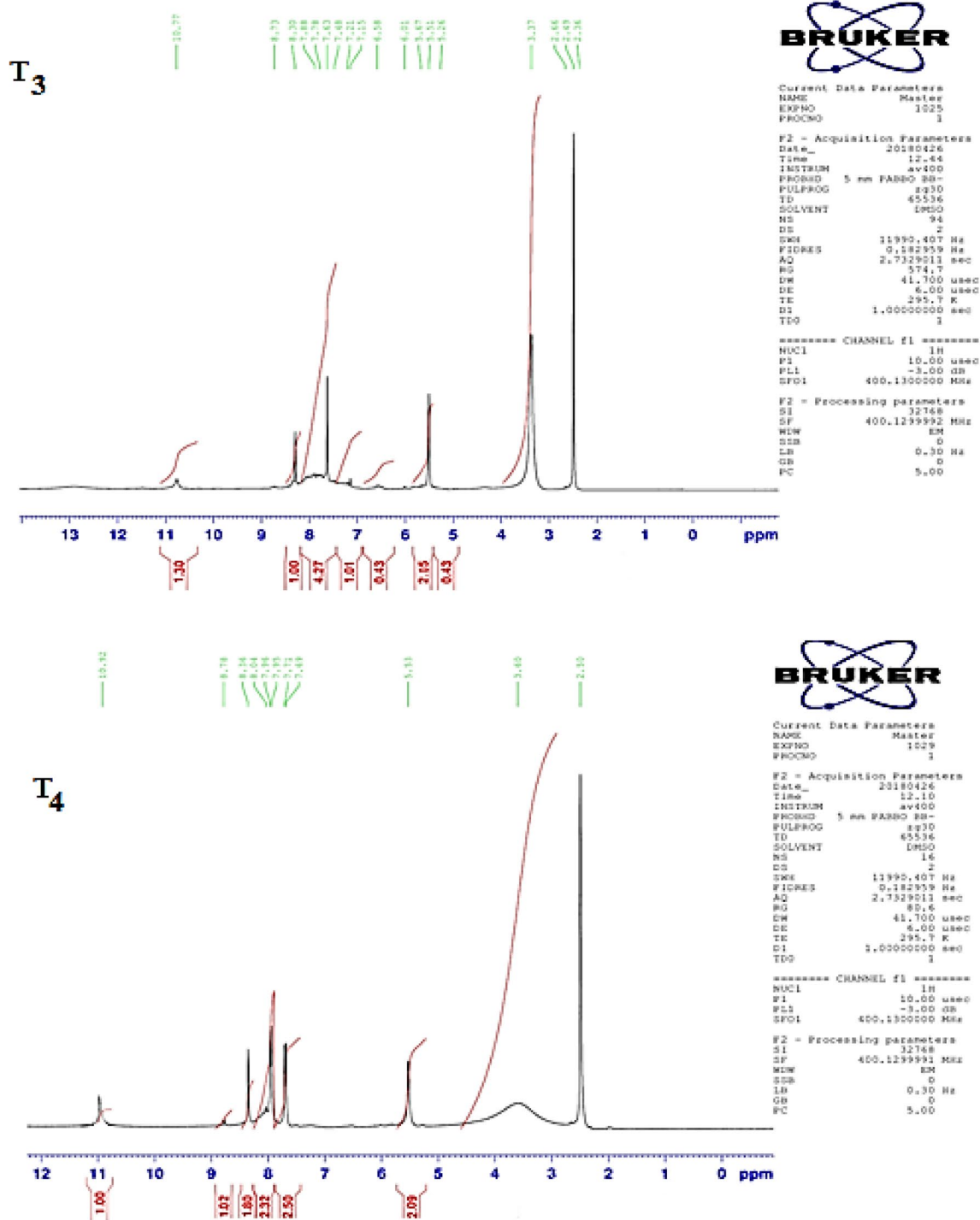
Fig. 3 (continued)

The average value of standard adsorption free energy was -34.85 kJ/mol. The negative value of $\Delta G_{ads}°$ ensures the spontaneous adsorption process and stability of the adsorbed layer on the metal surface. Commonly, the value of $\Delta G_{ads}°$ up to -20 kJ/mol is consistent with electrostatic interaction between the charged molecules and the charged metal (physical adsorption), while those around -40 kJ/mol or higher are associated with chemical adsorption as a result of sharing or transfer of electrons from the molecules to the metal surface to form a coordinate type of bond [32]. However, other researchers suggested that the range of standard adsorption free energy of chemical adsorption processes for
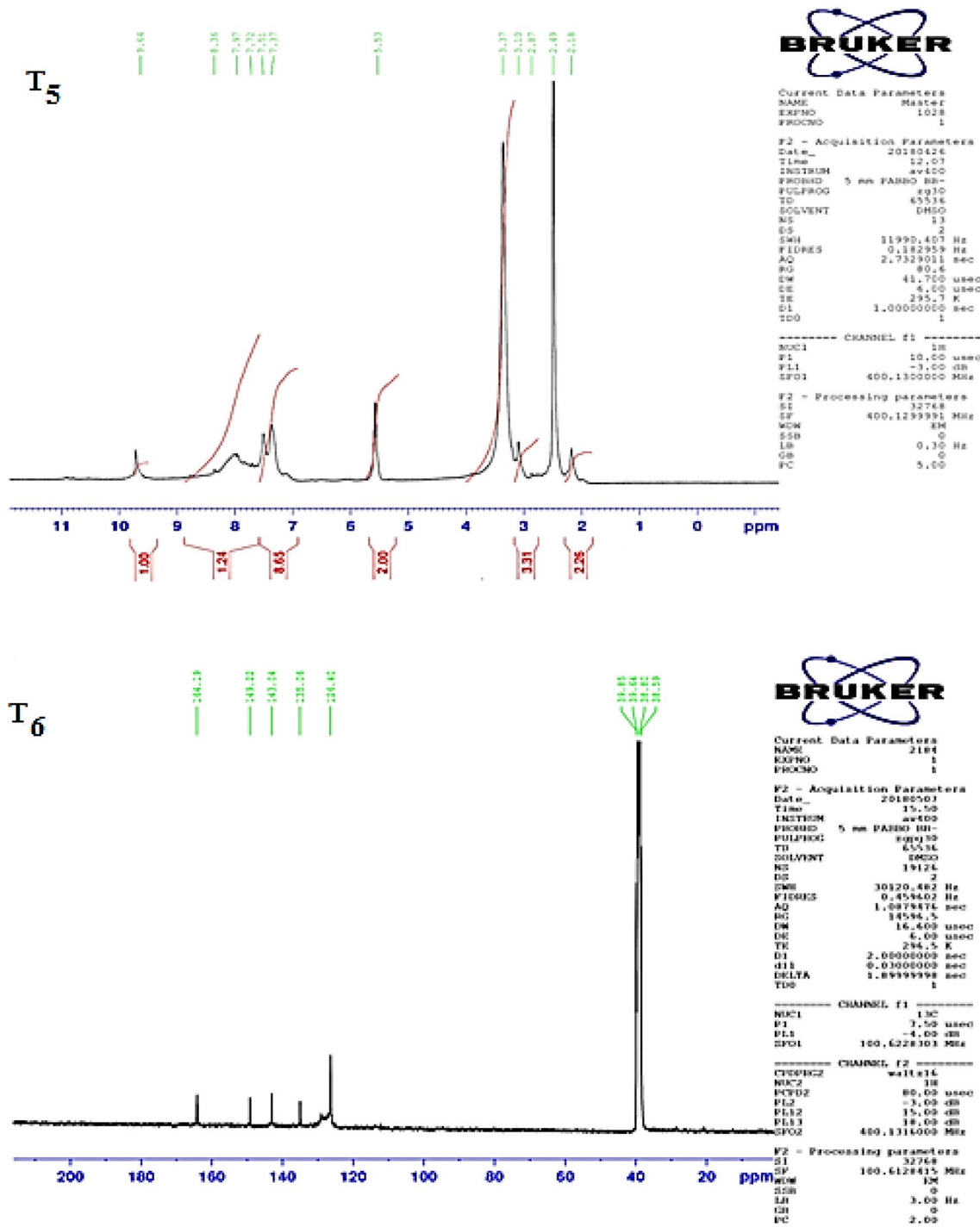
Fig. 3 (continued)

inhibitor in aqueous media lies between -21 and -42 kJ/mol [33]. Therefore, for the present work the values of adsorption heat have been considered within the range of chemical adsorption. As can also be observed from Table 4, there is a limited increase in the absolute value of ΔG_{ads} with an increase in temperatures, indicating that the adsorption was somewhat favorable with increasing experimental temperature and T_4 adsorbed according to chemical mechanism.

Table 1 Physical property of the synthesis compounds

Inhibitor	m.p. (°C)	Color	Molecular formula	Res. solvent	% Yield
T_1	231–233	Deep brown	$C_8H_8N_4O_2S$	Ethanol/water	67
T_2	193–195	Yellow	$C_7H_7N_5S$	Ethanol/water	70
T_3	˃300	Deep brown	$C_{22}H_{16}N_8O_4S$	Ethanol/water	78
T_4	263–265	Green	$C_{24}H_{20}N_{10}S_2$	Ethanol/water	76
T_5	287–289	Yellow	$C_{17}H_{15}N_9S_2$	Ethanol/water	70
T_6	207–209	Orange	$C_{20}H_{19}N_7OS$	Ethanol/water	64

Table 2 Corrosion rate of low-carbon steel alloy and inhibitor efficiency of synthesis compounds corrosion in 0.5 M hydrochloric acid solution at 30 °C and 0.001 M inhibitor concentration

Inhibitor	Formula	Corrosion rate (g/m^2 day)	Inhibitor efficiency (%)	Standard deviation (SD)
T_1	$C_8H_8N_4O_2S$	17.22	75.79	0.181
T_2	$C_7H_7N_5S$	18.55	76.95	0.195
T_3	$C_{22}H_{16}N_8O_4S$	21.61	73.16	0.227
T_4	$C_{24}H_{20}N_{10}S_2$	15.23	81.08	0.159
T_5	$C_{17}H_{15}N_9S_2$	35.16	78.16	0.369
T_6	$C_{20}H_{19}N_7OS$	21.82	72.89	0.229

3.4 Effect of Temperature and Activation Studies

As shown in Table 5, at specific experimental temperature, corrosion rate of steel decreases with an increase in T_4 concentration. The kinetics of the T_4 action can be realized by comparing the activation parameters in the presence and absence of the inhibitor. Activation energy (E_a), enthalpy of activation (ΔH_a), and entropy of activation (ΔS_a) for both uninhibited and inhibited 0.5 M hydrochloric acid steel corrosion at different temperatures and acid concentration were evaluated from an Arrhenius-type plot (Eq. 5) and transition state theory (Eq. 6) [33]:

$$CR = A \exp\left(-\frac{E_a}{RT}\right) \tag{5}$$

Table 3 Corrosion rate of low-carbon steel alloy and inhibitor efficiency of synthesis T_4 in 0.5 M hydrochloric acid solution at different conditions

Test number	Inhibitor concentration (M)	Temperature (°C)	Corrosion rate (g/m^2 day)	Inhibitor efficiency (%)	Standard deviation (SD)
1	0	20	75.39	–	1.938
2	0	30	80.52	–	2.138
3	0	40	154.79	–	2.032
4	0	50	420.05	–	3.371
5	1×10^{-3}	20	10.29	86.35	0.401
6	2×10^{-3}		7.78	89.67	0.303
7	3×10^{-3}		7.35	90.24	0.286
8	4×10^{-3}		6.14	91.84	0.239
9	1×10^{-3}	30	15.33	80.95	0.597
10	2×10^{-3}		15.23	81.08	0.593
11	3×10^{-3}		13.43	83.31	0.523
12	4×10^{-3}		10.78	86.61	0.421
16	1×10^{-3}	40	21.17	86.32	0.825
14	2×10^{-3}		21.04	86.4	0.821
15	3×10^{-3}		20.97	86.45	0.817
16	4×10^{-3}		16.39	89.4	0.639
17	1×10^{-3}	50	27.89	93.35	1.087
18	2×10^{-3}		17.89	95.74	0.697
19	3×10^{-3}		16.81	95.99	0.655
20	4×10^{-3}		16.68	96.02	0.651

Fig. 4 Langmuir adsorption isotherms of T_4 on the steel surface in 0.5 M HCl solution at different temperatures

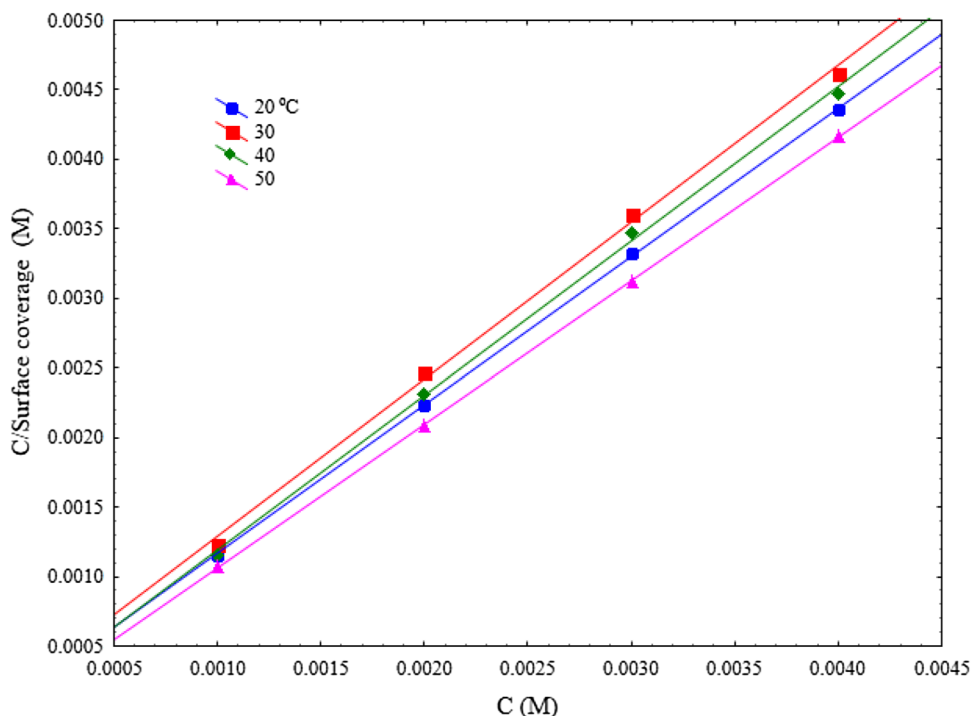

Table 4 Adsorption parameters of T_4 at different temperatures

T (°C)	K (M^{-1})	Slop	R^2	ΔG_{ads} (kJ/mol)
20	10471.2	1.07	0.99	− 32.33
30	11005.4	1.13	0.99	− 33.56
40	12706.5	1.11	0.99	− 35.04
50	30303.3	1.03	0.99	− 38.49
Average value	16121.6	1.09	0.99	− 34.85

Table 5 Activation parameters for steel corrosion reaction in uninhibited and inhibited 0.5 M HCl

C (M)	A (gmd)	E_a (kJ/mol)	ΔH_a (kJ/mol)	ΔS_a (J/mol K)
0	6.5×10^9	45.18	42.63	− 65.02
1×10^{-3}	4.7×10^5	26.12	23.56	− 144.33
2×10^{-3}	1.1×10^5	22.61	20.05	− 157.23
3×10^{-3}	1.3×10^5	23.44	20.88	− 155.06
4×10^{-3}	4.7×10^5	27.15	24.58	− 144.41

$$\mathrm{CR} = \frac{RT}{Nh} \exp\left(\frac{\Delta S_a}{R}\right) \exp\left(-\frac{\Delta H_a}{RT}\right), \tag{6}$$

where CR is the corrosion rate, A is the Arrhenius constant, R is the universal gas constant, h is Plank's constant, and N is Avogadro's number. As shown in Fig. 5, plot of ln(CR) versus $1/T$ gives straight lines with slopes of $\Delta E_a/R$ and intercept can be used for evaluating A, while Fig. 6 shows a liner straight lines of ln(CR/T) versus $1/T$ slopes of $\Delta H_a/R$ and intercept can be used for evaluating ΔS_a. Table 5 illustrates the activation parameters for steel corrosion reaction acidic solution at different conditions. It is clearly shown that the activation energy and enthalpy vary in a similar way. The activation energy and activation enthalpy for uninhibited acid were higher than the inhibited one. The decrease in the value of activation energy and enthalpy appears to be unreliable. However, this may be attributed to the increase of metal surface coverage by the inhibitor molecules at higher temperatures and also suggested that the formation rate of the chemisorbed layer may be greater than its rate of dissolution at higher temperatures [34]. Other researchers [35] found that some anticorrosion materials in the acidic solutions alter the kinetics of corrosion reaction by proposing alternate reaction paths with lower activation energies. Table 5 illustrates also that all the values of frequency factor are lower than uninhibited one, which is benefit for inhibiting the corrosion rate of steel. It is also well known that the increase in A raises the corrosion rate of steel [36]. Furthermore, at all cases, the values of E_a are higher than ΔH_a by a value which is approximately equal to RT, which confirm the thermodynamic principle of the reactions is characterized by the following equation [37]:

$$E_a - \Delta H_a = RT \tag{7}$$

The negative value of ΔS_a for both cases of the absence and presence of inhibitor indicates that activated complex in the rate-determining step denotes an association rather than a dissociation step, which means a decrease in

Fig. 5 Arrhenius plots of steel in uninhibited and inhibited 0.5 M HCl
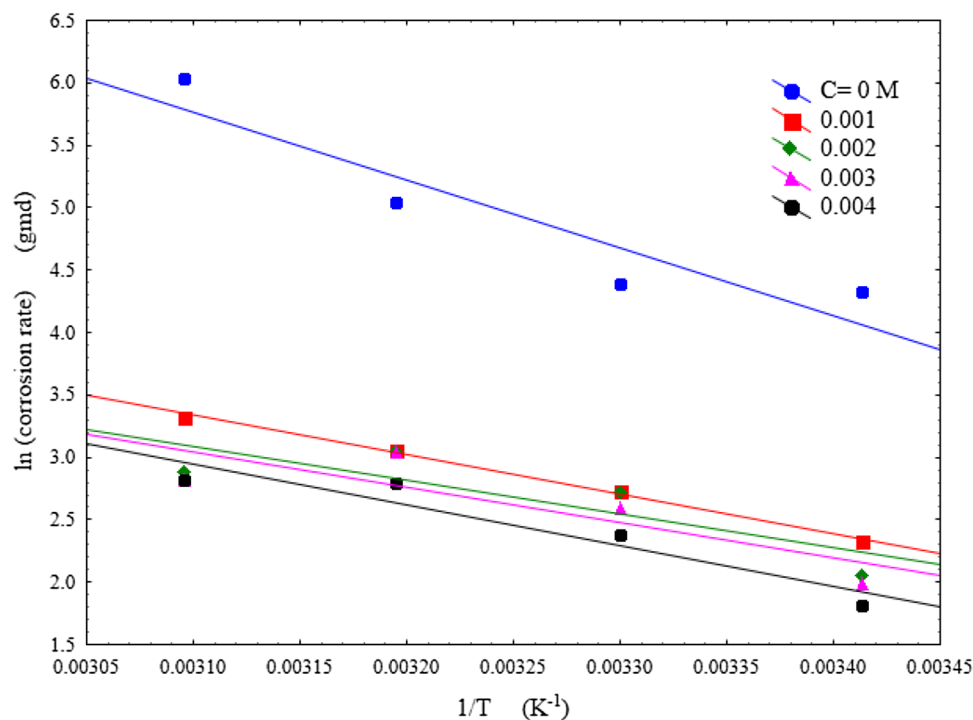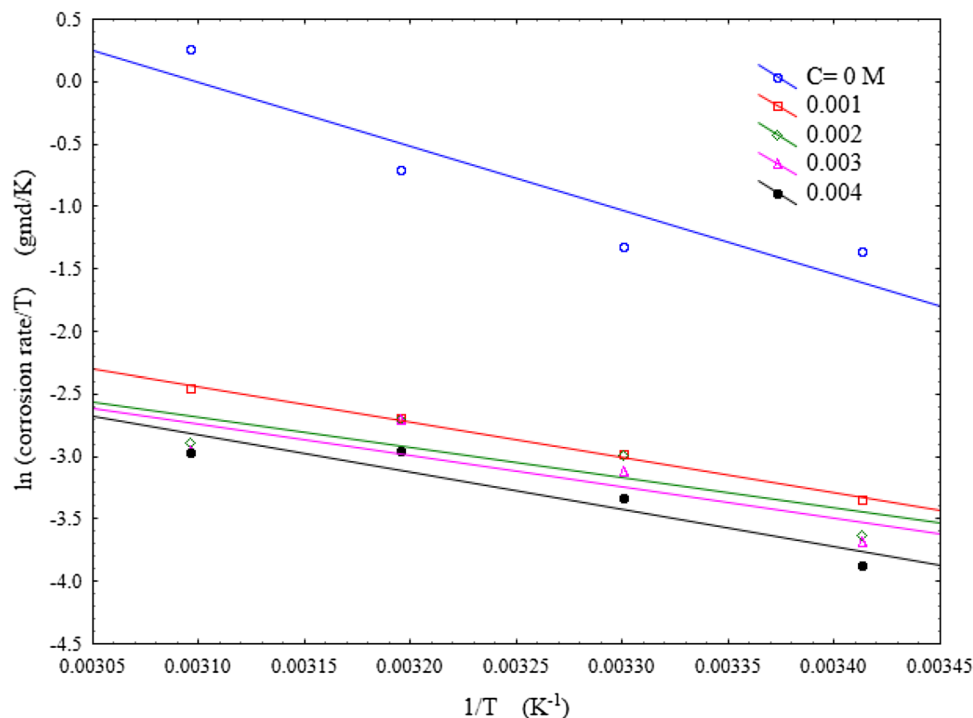

Fig. 6 Transition–state plots of steel in uninhibited and inhibited 0.5 M HCl

disorder takes place during the course of transition from reactant to the activated complex [38].

3.5 Quantum Chemical and Theoretical Calculations

Calculations of quantum chemical have been widely used to investigate reaction mechanism of inhibition process

[39]. It is also verified to be a very important tool for studying corrosion control mechanism and to obtain insight view to the inhibition mechanism of inhibitors. By using quantum chemical calculations, the structural parameters, such as HOMO (highest occupied molecular orbital), LUMO (lowest unoccupied molecular orbital),
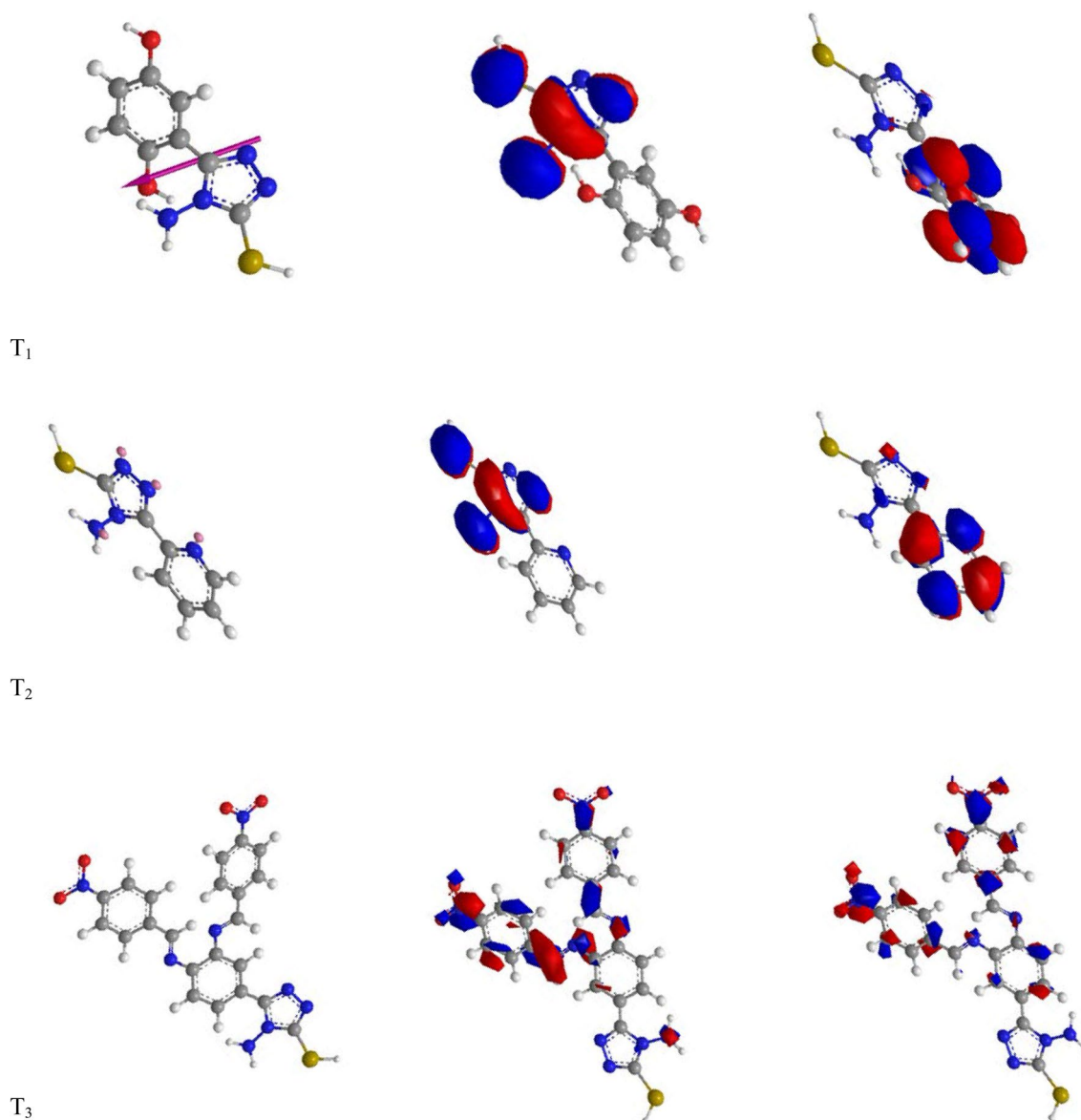
T_1

T_2

T_3

Fig. 7 Optimized structure of inhibitors

dipole moment (μ), and fraction of electron transferred (ΔN), were calculated. Figure 7 shows the optimized structures, HOMO and the LUMO structure of all synthesis inhibitors. The calculated quantum chemical properties are summarized in Table 6. As shown in Fig. 7, both the HOMO and LUMO distributions of synthesis inhibitors were concentrated mainly over sulfur and nitrogen atoms. E_{LUMO} and E_{HOMO} characterized the electron-receiving and electron-donating capability of synthesis inhibitors. In general, a low E_{LUMO} implies that inhibitors tend to accept electrons, while a high E_{HOMO} refers to a strong electron-donating [40]. Energy gap (ΔE) specifies the chemical stability of inhibitors, and a lower energy gap value typically leads to higher adsorption on the metal surface, resulting

in greater inhibition efficiencies [41]. The order of energy gap was $T_4 > T_5 > T_2 > T_1 > T_3 > T_6$, which is in agreement with the order of the inhibition efficiency that is obtained from experimental studies.

The number of transferred electrons (ΔN) was also calculated according to Eq. 8 [42]

$$\Delta N = \frac{X_{Fe} - X_{inh}}{2(\eta_{Fe} + \eta_{inh})}, \tag{8}$$

where X_{Fe} and X_{inh} denote the absolute electronegativity of iron and the inhibitor molecules, respectively; η_{Fe} and η_{inh} denote the absolute hardness of iron and the inhibitor molecule, respectively. These quantities are related to electron
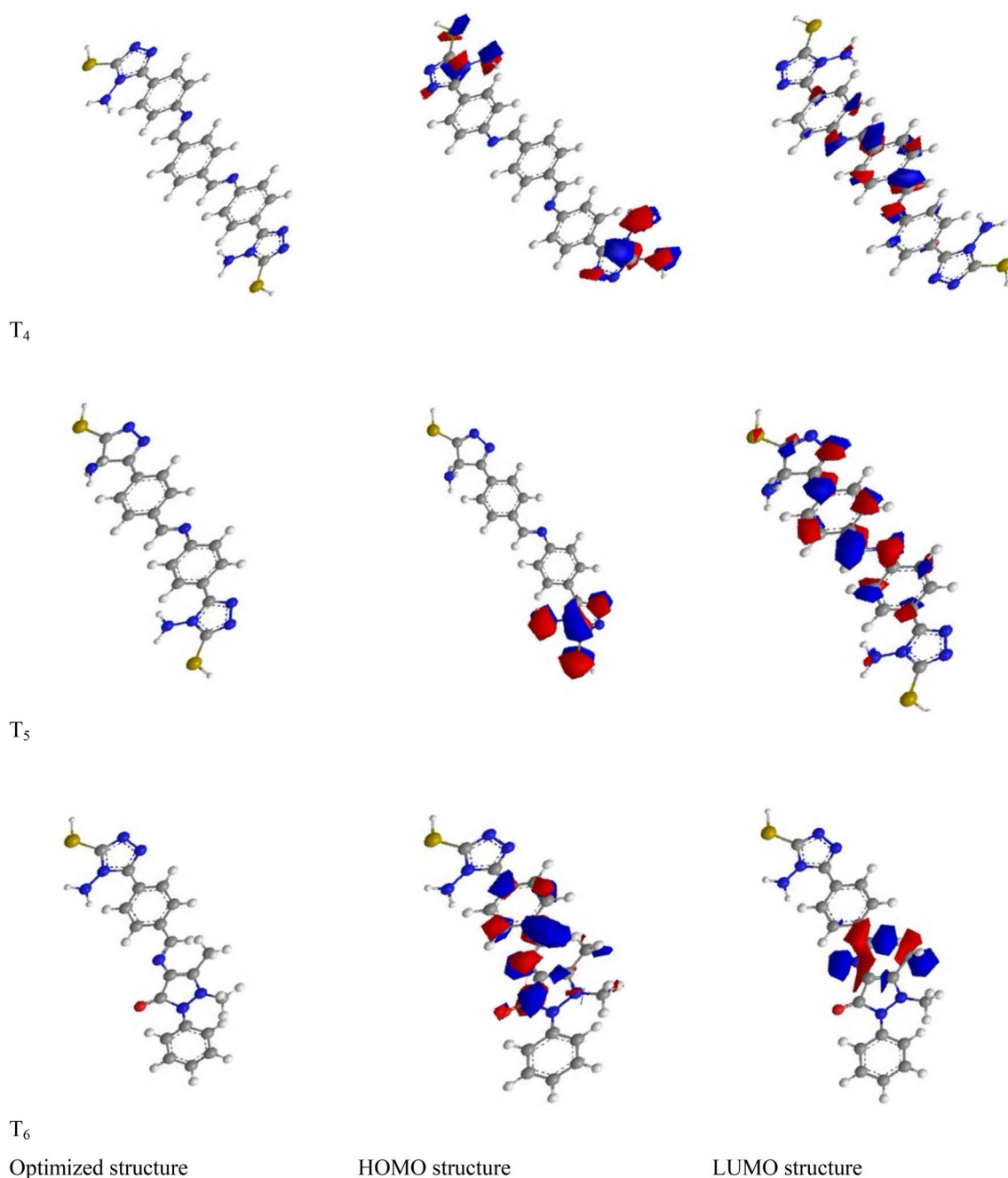
T₄

T₅

T₆

| Optimized structure | HOMO structure | LUMO structure |

Fig. 7 (continued)

affinity (A) and ionization potential (I) that are both related in turn to E_{HOMO} and E_{LUMO}:

$$X = \frac{I + A}{2} = \frac{-(E_{HOMO} + E_{LUMO})}{2}$$
$$\eta = \frac{I - A}{2} = \frac{-(E_{HOMO} - E_{LUMO})}{2}.$$

(9)

Values of X and η were considered using the values of I and A gained from quantum chemical calculation. The theoretical value of X_{Fe} is 7 according to Pearson's electronegativity scale and η_{Fe} is 0 eV/mol, respectively [43]. The fraction of electrons transferred from inhibitor to the steel surface (ΔN) was calculated and is listed in Table 6. According to Lukovits [44], if $\Delta N < 3.6$, the inhibition efficiency increased with increasing electron-donating ability at the steel surface. In this study, synthesis inhibitors were

Table 6 Calculated quantum chemical parameters of prepared inhibitors

Compounds	E_{HOMO} (eV)	E_{LUMO} (eV)	ΔE (eV)	ΔN	μ (Debye)
T_1	−7.828	−5.236	2.592	0.185	5.113
T_2	−7.690	−5.716	1.974	0.151	6.643
T_3	−7.840	−1.318	6.522	0.371	4.350
T_4	−6.981	−5.711	1.271	0.515	11.16
T_5	−5.551	−2.728	2.823	1.013	6.916
T_6	−7.675	−0.606	7.069	0.405	3.174

the donor of electrons, and the metal surface was the acceptor. This result supports the assertion that the adsorption of inhibitors on the surface of steel can occur on the bases of donor–acceptor interactions between the Л electrons of the compound and the vacant *d*-orbitals of the steel surface. The dipole moment (μ) is also a significant factor and there is a lack of agreement on the relation between μ and inhibitive performance. Some researchers found that a low μ value will favor accumulation of the inhibitor on metal surface and increasing the inhibitor performance [45, 46]. While other researchers suggested that a high value of dipole moment associated to the dipole–dipole interaction of inhibitor and metal surface can enhance the adsorption on the metal surface and increasing efficiency [47, 48]. In the present work, the value of μ for T_4 was the higher one among all tested inhibitors that agree with the second opinion. This may be attributed to the fact that O, N, S, and some C atoms have high charge densities. The regions of the highest electron density are commonly the sites to which electrophiles can attach [49, 50]. Therefore, these atoms are the active centers, which have the high capacity to bond to the steel surface. The relative higher efficiency of T_4 may be attributed to higher number of carbon atoms as compared with other inhibitors.

Khaled [51] used molecular simulation technique to optimize the structure of triazole derivatives as a corrosion inhibitor for iron. Experimental and theoretical data showed that aminotriazole was the best inhibitor among triazole, aminotriazole, and benzotriazole. Babić-Samardžija and Hackerman [52] also applied molecular modeling to get insights into structural and electronic effects of polypyrazolylborates, dihydrobis(1-pyrazolyl) borate, and hydrotris(1-pyrazolyl)borate in relation to their adsorption behavior and inhibition efficiencies. According to the findings of their electrochemical measurements, both polypyrazolylborates were relatively efficient inhibitors against acidic iron corrosion. Lebrini et al. [53] studied the influence of 2,5-bis(4-pyridyl)-1,3,4-thiadiazole (4-PTH) and some of its derivatives on the corrosion of mild steel in acidic media by quantum chemical method. The HOMO energy and LUMO energy and dipole moments were evaluated.

These parameters were correlated in a model with correlation coefficient higher than 0.93 that indicated a good relation between the corrosion inhibition and the structure of the inhibitors. Sahin et al. [54] studied the dependence of inhibition efficiencies of three heterocyclic compounds using the quantum chemical method. Parameters, such as the LUMO and HOMO energies, net atomic charges, energy gap, dipole moments, total and interaction energies, were calculated. A good agreement was found between theoretical and experimental data.

4 Conclusion

The following points can be concluded from the present work:

1. The six inhibitors were synthesized and tested successfully as corrosion inhibitors for steel in acidic solution.
2. Experimental results show that the order of inhibition efficiency was $T_4 > T_5 > T_2 > T_1 > T_3 > T_6$.
3. The addition of T_4 to the 0.5 M HCl solution at different temperatures and inhibitor concentration reduces corrosion of mild steel with inhibitor efficiency exceeding 96.02%.
4. Inhibitor efficiency of T_4 increased with an increase in the inhibitor concentration. The high inhibition efficiency of inhibitor was attributed to the formation of a layer on the steel surface.
5. Adsorption follows Langmuir adsorption isotherm with high negative value of heat of adsorption, which indicates the formation of chemical layer on metal surface.
6. Experimental studies were confirmed and agreed with theoretical quantum chemical calculations.

Compliance with Ethical Standards

References

1. Benabdellah M, Yahyi A, Dafali A, Aouniti A, Hammouti B, Ettouhami A (2011) Corrosion inhibition of steel in molar HCl by triphenyltin2–thiophene carboxylate. Arab J Chem 4:343
2. Zhang F, Tang Y, Cao Z, Jing W, Wu Z, Chen Y (2012) Performance and theoretical study on corrosion inhibition of

2-(4-pyridyl)-benzimidazole for mild steel in hydrochloric acid. Corros Sci 61:1

3. Shukla SK, Quraishi MA (2009) 4-Substituted anilinomethylpropionate: new and efficient corrosion inhibitors for mild steel in hydrochloric acid solution. Corros Sci 51:1990–1997

4. Khadom A, Abd A, Ahmed N (2018) Potassium iodide as a corrosion inhibitor of mild steel in hydrochloric acid: kinetics and mathematical studies. J Bio Tribo Corros 4:17

5. Bentiss F, Jama C, Mernari B, El Attari H, El Kadi L, Lebrini M, Traisnel M, Lagrenée M (2009) Corrosion control of mild steel using 3,5-bis(4-methoxyphenyl)-4-amino-1,2,4-triazole in normal hydrochloric acid medium. Corros Sci 51:1628–1635

6. Mahdavian M, Ashhari S (2010) Corrosion inhibition performance of 2-mercaptobenzimidazole and 2-mercaptobenzoxazole compounds for protection of mild steel in hydrochloric acid solution. Electrochim Acta 55:1720–1724

7. Musa AY, Kadhum AAH, Mohamad AB, Takriff MS (2010) Experimental and theoretical study on the inhibition performance of triazole compounds for mild steel corrosion. Corros Sci 52:3331–3340

8. Zarrok H, Saddik R, Oudda H, Hammouti B, El Midaoui A, Zarrouk A, Benchat N, EbnTouhami M (2011) 5-(2-Chlorobenzyl)-2, 6-dimethylpyridazin-3-one: an efficientInhibitor of C38 steel corrosion in hydrochloric acid. Pharma Chem 3(5):272–282

9. Ju H, Kai ZP, Li Y (2008) Aminic nitrogen-bearing polydentate Schiff base compounds as corrosion inhibitors for iron in acidic media: a quantum chemical calculation. Corros Sci 50:865–871

10. Masoud MS, Awad MK, Shaker MA, El-Tahawy MMT (2010) The role of structural chemistry in the inhibitive performance of some aminopyrimidines on the corrosion of steel. Corros Sci 52:2387–2396

11. Chen W, Luo HQ, Li NB (2011) Inhibition effects of 2,5-dimercapto-1,3,4-thiadiazole on the corrosion of mild steel in sulphuric acid solution. Corros Sci 53:3356–3365

12. Doner A, Solmaz R, Özcan M, Kardas G (2011) Experimental and theoretical studies of thiazoles as corrosion inhibitors for mild steel in sulphuric acid solution. Corros Sci 53:2902–2913

13. Obi-Egbedi NO, Obot IB, El-Khaiary MI, Umoren SA, Ebenso EE (2011) Computational simulation and statistical analysis on the relationship between corrosion inhibition efficiency and molecular structure of some phenanthroline derivatives on mild steel surface. Int J Electrochem Sci 6:5649–5675

14. Aljourani J, Golozar MA, Raeissi K (2010) The inhibition of carbon steel corrosion in hydrochloric and sulfuric acid media using some benzimidazole derivatives. Mater Chem Phys 121(1–2):320–325

15. Abboud Y, Abourriche A, Saffaj T, Berrada M, Charrouf M, Bennamara A, Himidi NA, Hannache H (2007) 2,3-Quinoxalinedione as a novel corrosion inhibitor for mild steel in 1 M HCl. Mater Chem Phys 105(1):1–5

16. Quraishi MA, Sharma HK (2002) 4-Amino-3-butyl-5-mercapto-1,2,4-triazole: a new corrosion inhibitor for mild steel in sulphuric acid. Chem Phys 78:18–21

17. Kuznestov YI, Semiletov AM, Chirkunov AA (2016) Inhibition of magnesium corrosion by triazoles. Int J Corros Scale Inhib. https://doi.org/10.17675/2305-6894-2016-5-1-3

18. Abd El-Maksoud SA (2008) The effect of organic compounds on the electrochemical behaviour of steel in acidic media. Int J Electrochem Sci 3:528–555

19. Lokesh SV, Satpati AK, Sherigara BS (2010) Electrochemical behavior of 1,2,4-triazole and benzotriazole at glassy carbon electrode in acidic media. Open Electrochem J 2:15–21

20. Walker R (1980) Benzotriazole a corrosion inhibitor for antiques: Some practical surface chemistry. J Chem Educ 57:789

21. Satpati AK, Ravindran PV (2008) Electrochemical study of the inhibition of corrosion of stainless steel by 1,2,3-benzotriazole in acidic media. Mater Chem Phys 109:352–359

22. Khaled KF, Fadl-Allah SA, Hammouti B (2009) Some benzotriazole derivatives as corrosion inhibitors for copper in acidic medium: experimental and quantum chemical molecular dynamics approach. Mater Chem Phys 117(1):148–155

23. Arun K, Gupta S, Prachand A, Patel, Jain S (2012) Synthesis of some 4-amino-5-(substituted-phenyl)-4H-[1, 2, 4] triazole-3-thiol derivatives and Antifungal activity. Int J Pharm Life Sci 3:1848–1857

24. Aly AA, Brown AB, Talaatt I, El-Emary AM (2009) Hydrazine-carbothioamide group in the synthesis of heterocycles. ARKIVOC I:150–197

25. Khadom AA (2015) Kinetics and synergistic effect of halide ion and naphthylamin for inhibition of corrosion reaction of mild steel in hydrochloric acid. React Kinet Mech Catal 115:463–481

26. Khadom AA, Yaro AS (2011) Protection of low carbon steel in phosphoric acid by potassium iodide. Prot Met Phys Chem Surf 47:662–669

27. Chaitra TK, Mohana KN, Gurudatt DM, Tandon HC (2016) Inhibition activity of new thiazole hydrazones towards mild steel corrosion in acid media by thermodynamic, electrochemical and quantum chemical methods. J Taiwan Inst Chem Eng 67:521–531

28. Tezcan F, Yerlikaya G, Mahmood A, Kardaş G (2018) A novel thiophene Schiff base as an efficient corrosion inhibitor for mild steel in 1.0 M HCl: electrochemical and quantum chemical studies. J Mol Liq 269:398–406

29. Messali M, Larouj M, Lgaz H, Rezki N, Al-Blewi FF, Aouad MR, Chaouiki A, Salghi R, Chung I (2018) A new Schiff base derivative as an effective corrosion inhibitor for mild steel in acidic media: experimental and computer simulations studies. J Mol Struct 1168:39–48

30. Yaro AS, Khadom AA, Hadeel F, Ibraheem (2011) Peach juice as an anti-corrosion inhibitor of mild steel. Anti-Corros Methods Mater 58(3):116–124

31. Khadom AA, Yaro AS, AlTaie AS, Kadum AAH (2009) Electrochemical, activations and adsorption studies for the corrosion inhibition of low carbon steel in acidic media. Port Electrochim Acta 27(6):699–712

32. Ehteram A, Noor (2009) Evaluation of inhibitive action of some quaternary N-heterocyclic compounds on the corrosion of Al–Cu alloy in hydrochloric acid. Mater Chem Phys 114:533–541

33. Umoren SA, Ebenso EE (2007) The synergistic effect of polyacrylamide and iodide ions on the corrosion inhibition of mild steel in H_2SO_4. Mater Chem Phys 106:387–393

34. Musa AY, Kadhum AH, Mohamad AB, Takriff MS, Daud AR, Kamarudin SK (2010) On the inhibition of mild steel corrosion by 4-amino-5-phenyl-4H-1, 2, 4-trizole-3-thiol. Corros Sci 52:526–533

35. Putilova IN, Balezin SA, Barannik VP (1960) Metallic corrosion inhibitor. Pergamon Press, New York

36. El-Anadouli BE, Ateya BG, El-Nizamy FM (1986) The effect of temperature on the polarization resistance—I. Activation control. Corros Sci 26:419–424

37. Benabdellah M, Touzani R, Dafali A, Hammouti B, El Kadiri S (2007) Ruthenium–ligand complex, an efficient inhibitor of steel corrosion in H_3PO_4 media. Mater Lett 61:1197–1204

38. Noor EA, Al-Moubaraki AH (2008) Thermodynamic study of metal corrosion and inhibitor adsorption processes in mild steel/1-methyl-4 [4′(-X)-styryl pyridinium iodides/hydrochloric acid systems. Mater Chem Phys 110:145–154

39. Guo L, Zhu S, Zhang S, He Q, Li W (2014) Theoretical studies of three triazolederivatives as corrosion inhibitors for mild steel in acidic medium, Corros Sci 87:366–375

40. Zhang D, Tang Y, Qi S, Dong D, Cang H, Lu G (2016) The inhibition performance of long-chain alkyl-substituted benzimidazole derivatives for corrosion of mild steel in HCl. Corros Sci 102:517–522

41. Hu K, Zhuang J, Ding J, Ma Z, Wang F, Zeng X (2017) Influence of biomacromolecule DNA corrosion inhibitor on carbon steel. Corros Sci 125:68–76

42. Mourya P, Singh P, Tewari AK, Rastogi RB, Singh MM (2015) Relationship between structure and inhibition behaviour of quinolinium salts for mild steel corrosion: experimental and theoretical approach. Corros Sci 95:71–87

43. Pearson RG (1988) Absolute electronegativity and hardness: application to inorganic chemistry. Inorg Chem 27:734–740

44. Lukovits I, Lalman E, Zucchi F (2001) Corrosion inhibitors—correlation between electronic structure efficiency. Corrosion 57:3–8

45. Qiang Y, Guo L, Zhang S, Li W, Yu S, Tan J (2016) Synergistic effect of tartaric acidwith 2,6-diaminopyridine on the corrosion inhibition of mild steel in 0.5 M HCl. Sci Rep 6:33305

46. Li LJ, Zhang XP, Lei JL, He JX, Zhang ST, Pan FS (2012) Adsorption and corrosion inhibition of *Osmanthus fragran* leaves extract on carbon steel. Corros Sci 63:82–90

47. Yüce AO, Mert BD, Kardaş G, Yazıcı B (2014) Electrochemical andquantum chemical studies of 2-amino-4-methyl-thiazole as corrosioninhibitor for mild steel in HCl solution. Corros Sci 83:310–316

48. Zheng X, Zhang S, Li W, Gong M, Yin L (2015) Experimental and theoretical studiesof two imidazolium-based ionic liquids as inhibitors for mild steel in sulfuricacid solution. Corros Sci 95:168–179

49. Mahmmod AA, Kazarinov IA, Khadom AA et al (2018) Experimental and theoretical studies of mild steel corrosion inhibition in phosphoric acid using tetrazoles derivatives. J Bio Tribo Corros 4:58

50. Obot IB, Ebenso EE, Akpan IA, Gasem ZM, Alfobi Ayo S (2012) Thermodynamic and density functional theory investigation of sulphathiazole as green corrosion inhibitor at mild steel/hydrochloric acid interface. Int J Electrochem Sci 7:1978–1996

51. Khaled KF (2008) Molecular simulation, quantum chemical calculations and electrochemical studies for inhibition of mild steel by triazoles. Electrochim Acta 53:3484–3492

52. Babić-Samardžija K, Hackerman N (2006) Iron corrosion inhibition with dihydrobis- and hydrotris-(1-pyrazolyl)borates. Anticorros Methods Mater 53:19–29

53. Lebrini M, Bentiss F, Vezin H, Lagrenee M (2006) The inhibition of mild steel corrosion in acidic solutions by 2,5-bis(4-pyridyl)-1,3,4-thiadiazole: structure-activity correlation. Corros Sci 48:1279–1291

54. Şahin M, Gece G, Karcı F, Bilgic S (2008) Experimental and theoretical study of the effect of some heterocyclic compounds on the corrosion of low carbon steel in 3.5% NaCl medium. J Appl Electrochem 38:809–815